Thin Solid Films 517 (2009) 5981–5987

Contents lists available at ScienceDirect

Thin Solid Films

journal homepage: www.elsevier.com/locate/tsf

Electrochemical deposition of zinc selenide and cadmium selenide onto porous silicon from aqueous acidic solutions

E.B. Chubenko *, A.A. Klyshko, V.A. Petrovich, V.P. Bondarenko

Department of Micro and Nanoelectronics, Belarusian State University of Informatics and Radioelectronics, Minsk 220013, Belarus

ARTICLE INFO

Article history:
Received 16 December 2008
Received in revised form 13 March 2009
Accepted 17 March 2009
Available online 24 March 2009

Keywords:
Electrochemical deposition
Selenides
Porous silicon
X-ray diffraction
Voltammetry

ABSTRACT

An electrochemical deposition process of ZnSe and CdSe compound semiconductors from aqueous acidic solutions onto silicon substrates with porous silicon layers formed on their surfaces was studied by the voltammetry method. The experimental data obtained were compared with the deposition data onto metal and silicon substrates, and the optimal conditions for the binary compound deposition onto porous silicon were determined. Semiconductor films deposited were studied by scanning electron microscopy, X-ray diffractometry, and X-ray microanalysis. The films are shown to have the crystalline structure and a nearly stoichiometric composition with a minor Se excess. Further annealing in air for 15 min allowed the Se concentration to be decreased.

1. Introduction

Recent microelectronic technology is dominated by exclusively silicon. But at the same time other materials occupy leading place in manufacture of optoelectronic, electromagnetic, etc. devices. An epitaxial growth of high-quality layers of dissimilar materials on a Si substrate would make it possible to combine the multitude of various devices with Si electronic circuits into a compact, reliable, and cheap system. Wide-band II–VI compound semiconductors such as ZnSe and CdSe are in considerable optoelectronic use as a material for active layers of solar cells, light diodes, laser diodes, photo- and electro-luminescent devices [1,2]. However, mismatch of the crystal lattice constants (for example 4.4% for ZnSe and 11.4% for CdSe) and ~300% difference in thermal expansion coefficients prohibit the epitaxial growth of these semiconductors on silicon.

Porous silicon (PS) buffer layer permits the implementation of lattice-mismatched heteroepitaxial films on Si substrates. This idea was confirmed by the heteroepitaxial growth of GaAs [3], PbTe [4,5] and diamond [6] films on a PS/Si substrate.

An electrochemical deposition of compound semiconductors offers certain advantages over epitaxial growth methods. First of all, these are low temperature and low cost of the process as well as a possibility of a simultaneous treatment of large surfaces [7]. The composition, thickness and morphology of the films formed can be easily controlled by a variation of the electric parameters of the process. The electrochemical synthesis of various binary and ternary semiconductor compounds on metal (Ni, Ti) and semiconductor (GaAs, InP) substrates was reported in a series of articles [1,2,8–14].

2. Experimental details

The mechanism of the electrochemical deposition process of II–VI compound semiconductors involving the same metal but different chalcogen atoms as, for example, ZnSe and ZnTe, is known to be practically the same. In the case when the above semiconductors involve the same chalcogen but different metal atoms, as ZnTe and CdTe, the deposits formed show different surface morphology and structure [7]. So, two binary compounds, ZnSe and CdSe, including atoms of different metals were chosen for our experiments.

The processes of the ZnSe and CdSe electrochemical deposition were studied by the voltammetry method. A thermostatically controlled three-electrode glass electrochemical cell with a magnetic stirrer was used at that. A potential scanning was performed with the PI-50-1.1 potentiostat attached to computer through the Advantech PCI-1710HG analog-to-digital converter. A commercial Ag/AgCl electrode was used as a reference electrode. The voltammograms of nickel (Ni), silicon (Si), and PS working electrodes were recorded. This allowed the features of the ZnSe and CdSe electrochemical deposition onto semiconductor substrates in comparison with that onto metal substrates to be revealed.

The surface of the Ni electrodes was cleaned in acetone with further bright etching for 10 s in a solution containing 85 ml H_3PO_4 and 15 ml HNO_3 at 100 °C. Then electrodes were rinsed in distilled water. Reproducibility of the Ni electrodes was controlled by checking of the equilibrium potential in the working electrochemical bath. Before the voltammogram recording, the n^+-type antimony-doped Si (100) electrodes of 0.01 Ω·cm resistivity were immersed into 4.5%

* Corresponding author.
E-mail address: eugene.chubenko@gmail.com (E.B. Chubenko).

0040-6090/$ – see front matter © 2009 Elsevier B.V. All rights reserved.
doi:10.1016/j.tsf.2009.03.134

hydrofluoric acid for 5 s to remove a native oxide film. The PS layers were formed on the n^+-type antimony-doped Si (100) substrates of 0.01 Ω·cm resistivity in the HF:H_2O:C_3H_7OH = 1:3:1 electrolyte with 9% HF at the anodization current density of 60 mA/cm^2. Porosity of the PS layer was 55% and the thickness was 2 μm. The thickness of the PS layers was measured on wafer cross-section with optical microscope LOMO MII-4. The porosity of the PS was determined by gravimetrical method.

In the case of the ZnSe deposition, $ZnSO_4$ and SeO_2 of analytical grade were used for the solution preparation. In the case of the CdSe deposition, $CdSO_4 \cdot 4H_2O$ and SeO_2 of analytical grade were used. In both cases appropriate quantity of the reagents was dissolved in distilled water. The concentration of the reagents varied for different experiments. pH of the solutions at a given temperature was normalized to needed value by the addition of sulfuric acid. Aqueous 0.1 M Na_2SO_4 solution was used as a stock electrolyte.

The surface morphology and composition of the deposited selenide films were studied by scanning electron microscopy (SEM) and X-ray microanalysis using the Cambridge Instruments Stereoscan-360 electron microscope, operating at 20 kV acceleration voltage, with Link Analytical AN 10000 integral spectrum analyzer. The phase composition of the films was studied by X-ray diffractometry (XRD) with the DRON-3 apparatus manufactured by RPE "Bourevestnik" Inc. (Russia).

3. Results and discussions

3.1. Thermodynamic conditions for the binary compound semiconductor deposition

According to the present concepts, the process of the electrochemical deposition of binary semiconductor compounds occurs by the mechanism of the so-called underpotential deposition [7]. Let us consider this mechanism for ZnSe and CdSe.

In acidic electrolytes, selenium deposits from the solution of selenium acid in accordance to the reaction:

$$SeO_3^{2-} + 6H^+ + 4e^- \rightarrow Se^0 + 3H_2O \quad (a)$$

The potential of this reaction relative to the Ag/AgCl electrode at 25 °C is equal to 0.52 V.

The zinc deposition takes place in accordance to the following reaction:

$$Zn^{2+} + 2e^- \rightarrow Zn^0, (-0.958 \text{Vvs.Ag/AgCl}) \quad (b)$$

But Zn can also be deposited via the interaction with adatoms of elementary selenium Se^0. The reaction is:

$$Zn^{2+} + Se^0 + 2e^- \rightarrow ZnSe \quad (c)$$

Gibbs free energy for the binary ZnSe compound is equal to $\Delta G_{ZnSe} = -137$ kJ/mole leads to a shift of the deposition potential of more inert Zn component by $\Delta E_{Zn} = 0.71$ V. So, in the ZnSe composition Zn may be deposited at potentials more positive than its equilibrium reduction potential in the range from −0.958 to −0.248 V.

Moreover, because difference between reduction potentials of compound components is equal to $\Delta E_{Se-Zn} = 0.52 - (-0.958) = 1.458$ V and it is more than the potential shift ΔE_{Zn}, the ZnSe deposition potential is determined by the Zn deposition potential all over the region of the binary compound deposition. At high deposition potentials (close to upper bound of the ZnSe deposition potential range) usually a selenium excess is observed, while at the excessively negative potentials a Zn excess takes place. A qualitative composition of the compound is also determined by the initial concentration of reagents in the solution. The best results can be obtained when the chalcogen concentration is 2–3 orders of magnitude less than the metal ion concentration [7].

The study of the electrochemical deposition of II–VI compound semiconductors is complicated due to the presence of side cathode reactions of hydrogen and hydrogen selenide H_2Se reduction [15] as well as by the influence of the surface condition [16]. These factors may limit a theoretical range of the deposition potential of compounds.

The above conclusions are true for cadmium selenide as well. Lower bound of the CdSe deposition potential range by the reaction

$$Cd^{2+} + Se^0 + 2e^- \rightarrow CdSe \quad (d)$$

is limited by the cadmium reduction potential in accordance with the reaction

$$Cd^{2+} + 2e^- \rightarrow Cd^0, (-0.625 \text{Vvs.Ag/AgCl}) \quad (e)$$

Gibbs free energy for the binary CdSe compound is equal to $\Delta G_{CdSe} = -100$ kJ/mole and a shift of the deposition potential of the metal Cd component is equal to 0.52 V. So, a theoretical range of the CdSe deposition potentials is within −0.625 and −0.105 V.

3.2. Voltammetry of the ZnSe formation process

Fig. 1 shows voltammograms of the nickel electrode in the electrolytes of various compositions. The voltammogram recorded in the stock 0.1 M Na_2SO_4 electrolyte (pH = 5, t = 25 °C) allowed value of the potential related to the reaction of the direct water electrolysis with the hydrogen formation to be determined. The voltammogram shows that this reaction occurs at the nickel electrode at the potential of about −1.2 V. At more positive potentials, no intense peaks associated with any cathode processes are observed. That is, this stock electrolyte may be reliably used to study the electrochemical ZnSe deposition since the reactions of our interest are expected at higher potentials.

The current density peaks at the potential of −1.3 V for the cathode polarization and at −0.8 V for the anode polarization related to the reduction and the dissolution of Zn^{2+} at the nickel electrode by the reaction (b) are well observed in the curve corresponding to the 0.15 M $ZnSO_4$ solution (pH = 4.5, t = 25 °C). The intensity of these peaks changes in proportion to the Zn^{2+} ion concentration in the solution (see inset in Fig. 1).

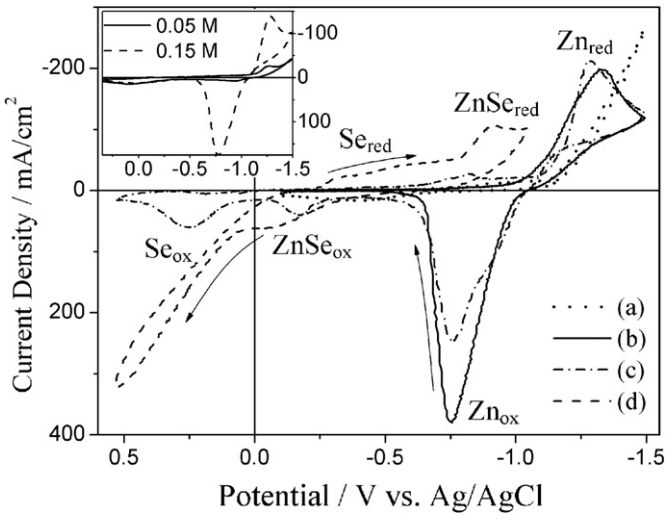

Fig. 1. Cyclic voltammograms of the Ni electrode in following aqueous solutions: (a) 0.1 M Na_2SO_4 at 25 °C, (b) 0.1 M Na_2SO_4 + 0.15 M $ZnSO_4$ at 25 °C, (c) 0.1 M Na_2SO_4 + 0.15 M $ZnSO_4$ + 10^{-3} M SeO_2 at 25 °C, and (d) 0.1 M Na_2SO_4 + 0.15 M $ZnSO_4$ + 10^{-3} M SeO_2 at 65 °C. Inset shows voltammograms of the Ni electrode in the 0.1 M Na_2SO_4 stock solution with a various concentration of Zn^{2+} ions. The scan rate is 2 V/s.

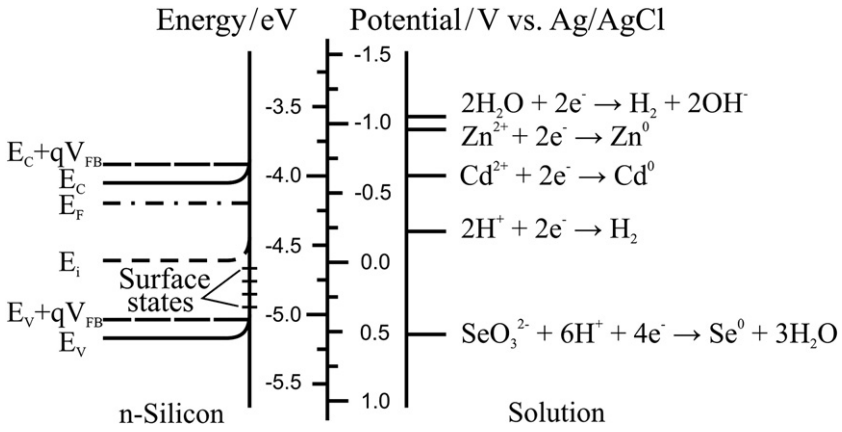

Fig. 2. A schematic band structure of the solution/silicon interface. pH and temperature dependences of potentials as well as superpotentials of cathode reactions are not considered. V_{FB} is a flat band voltage.

After adding of 0.001 M SeO_2 to the electrolyte, pH of the solution decreased to 2 and additional current density peaks were fixed. At the cathode polarization, the peak at about −0.8 V on the curve related to the temperature of 25 °C is followed by the constant current density region. This plateau (from −0.8 V to −1.1 V) corresponds to the binary semiconductor compound deposition by the mechanism described by the reaction (c).

At potentials lower than −1.1 V, the Zn deposition also takes place. This Zn deposit is dissolved at the anode polarization at the potential of −0.8 V. At the anode polarization, another two dissolution peaks are observed in the range of positive potentials. Maximum at the potential 0.3 V is related to the electrochemical Se dissolution while the appearance of the antecedent peak at the potential −0.2 V is caused by the ZnSe dissolution that was deposited onto Se at the cathode polarization.

The temperature increase to 65 °C resulted in the increase of the intensity of all peaks in the voltammogram. The peak related to the deposition of elementary Se appeared in the range prior to ZnSe deposition area. It should be noted that the Zn dissolution peak is absent in the last curve because in this case the potential was not scanned below −1 V, so the Zn deposition did not take place.

It should be taken into account in studies of the reactions at the semiconductor electrodes that not only the electrode surface condition exerts influence on these reactions but also the energy-band structure of semiconductor, specifically, band bending at the semiconductor/electrolyte interface. Since in most cases the electrochemical potentials of particles in the solution and in semiconductor are different, electron transfer between the system parts takes place when the silicon electrode is immersed into the solution, resulting in the formation of space-charge regions in both the solution and silicon, as shown in Fig. 2. The space-charge region in semiconductor usually is depleted with carriers, i.e. a barrier to electron transfer from semiconductor into electrolyte arises. So, without taking surface states at the semiconductor/electrolyte interface into account through which the electron exchange can take place, electrochemical reactions at the semiconductor electrode are possible only on reaching the flat band voltage. Magnitude of this voltage for silicon electrodes of n-type conductivity in solutions containing zinc sulphate and selenium oxide was not determined exactly. However, as further experiments showed, it is not high because no difficulties to the reactions observed at metal electrodes were revealed.

Fig. 3 demonstrates the cyclic voltammograms of the bulk n^+-Si electrode in various solutions. Referring to Fig. 3, typical peaks related to the hydrogen evolving are absent in the voltammogram of this electrode in the stock electrolyte, and the current increase conditioned by the direct water electrolysis is observed at the potentials more negative than at the nickel electrode. The reaction of the hydrogen formation is retarded due to the potential barrier at the electrode/electrolyte interface. The peak at the potential −1.3 V corresponding to the Zn deposition is not observed in the 0.1 M $ZnSO_4$ solution, however the peak of the Zn dissolution at the potential −0.8 V is observed. For the silicon electrode in the 0.1 M $ZnSO_4$ + 0.001 M SeO_2 electrolyte (pH = 2, t = 25 °C), there is a weak current increase in the voltammogram in the potential range where the electrochemical ZnSe deposition occurred at the metal electrode. So, the precipitation rate of the binary compound at the silicon electrode is very low.

When the electrolyte temperature was increased to 65 °C, the ZnSe precipitation rate increased considerably. The deposition range of the compound is the same as for nickel electrodes. However, referring to Fig. 3, in contrast to the nickel electrode, the current increase prior to the binary compound deposition and the peak related to the elementary Se reduction are absent in the voltammogram due to the potential barrier at the electrode/electrolyte interface. At the anode polarization, the peaks associated with the Se and ZnSe dissolution are not observed because in this case a height of the potential barrier at the silicon/electrolyte interface increases and there is difficulty in the carrier transfer through the interface. So, the undissolved deposit containing elementary Se and ZnSe remained at the silicon electrode during the voltammogram recording.

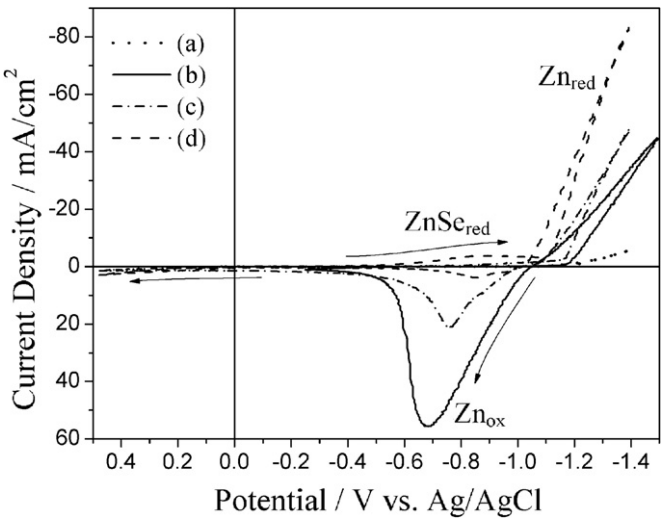

Fig. 3. Cyclic voltammograms of the bulk n^+ Si electrode in following aqueous solutions: (a) 0.1 M Na_2SO_4 at 25 °C, (b) 0.1 M Na_2SO_4 + 0.15 M $ZnSO_4$ at 25 °C, (c) 0.1 M Na_2SO_4 + 0.15 M $ZnSO_4$ + 10^{-3} M SeO_2 at 25 °C, and (d) 0.1 M Na_2SO_4 + 0.15 M $ZnSO_4$ + 10^{-3} M SeO_2 at 65 °C. The scan rate is 2 V/s.

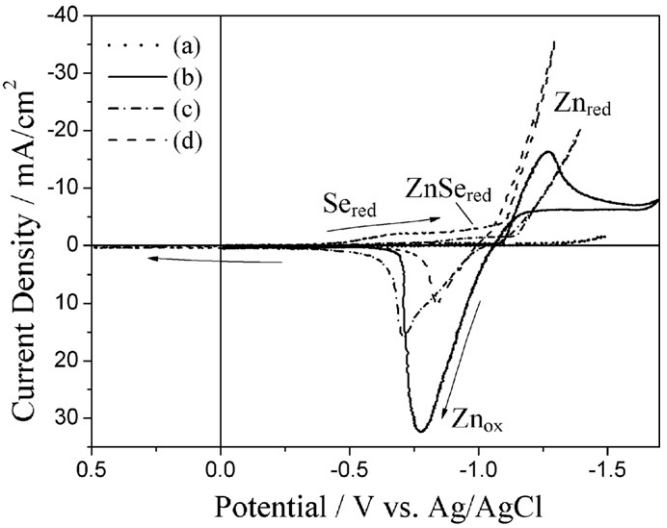

Fig. 4. Cyclic voltammograms of the PS electrode in following aqueous solutions: (a) 0.1 M Na_2SO_4 at 25 °C, (b) 0.1 M Na_2SO_4 + 0.15 M $ZnSO_4$ at 25 °C, (c) 0.1 M Na_2SO_4 + 0.15 M $ZnSO_4$ + 10^{-3} M SeO_2 at 25 °C, and (d) 0.1 M Na_2SO_4 + 0.15 M $ZnSO_4$ + 10^{-3} M SeO_2 at 65 °C. The scan rate is 1 V/s.

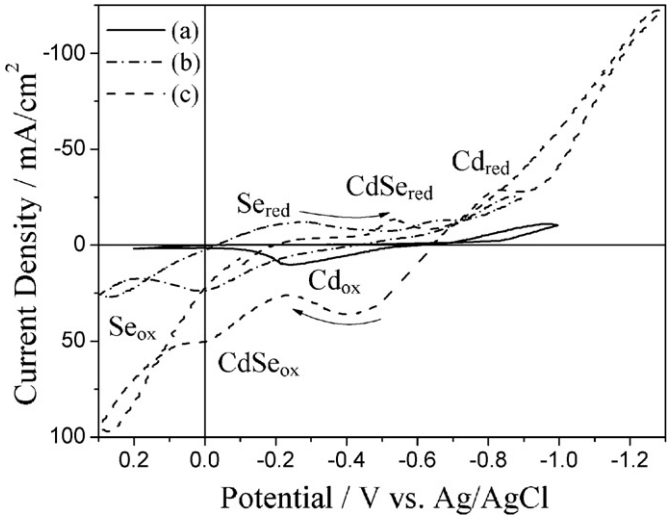

Fig. 5. Cyclic voltammograms of the Ni electrode in following aqueous solutions: (a) 0.01 M $CdSO_4$ at 25 °C, (b) 0.01 M $CdSO_4$ + 0.001 M SeO_2 at 25 °C, and (c) 0.01 M $CdSO_4$ + 10^{-5} M SeO_2 at 65 °C. The scan rate is 2 V/s.

Fig. 4 shows cyclic voltammograms of the PS electrode in various solutions. As shown in Fig. 4, in the voltammogram of this electrode in the stock 0.1 M Na_2SO_4 electrolyte at 25 °C, the reaction of the direct water electrolysis is observed at the same potentials as for the silicon electrode. In the voltammogram of this electrode in the 0.1 M $ZnSO_4$ electrolyte at 25 °C, we were able to register the peak related to the reduction of Zn^{2+} ions only with the reduced scan rate. Zn is deposited at the PS electrode also at the potential −1.3 V at the cathode polarization and is dissolved at the potential −0.8 V at the anode polarization.

In the voltammogram of the PS electrode in the solution for the ZnSe deposition (0.1 M $ZnSO_4$ + 0.001 M SeO_2, pH = 2) at 25 °C, a feebly marked current increase related to the binary compound deposition is observed in the range from −0.8 to −1 V. At the electrolyte temperature of 65 °C, a strongly pronounced plateau associated with the ZnSe deposition is observed at the cathode polarization. In this case, the potential was scanned only to −1.3 V, so the peak related to the Zn dissolution is less intensive than at 25 °C.

The current increase before the plateau of the binary compound deposition begins at more positive potentials for the PS electrode than for the silicon one. This can be conditioned by greater number of energy levels located in band gap, the appearance of which is caused by the surface states and defects of the strongly developed surface of PS. The peaks corresponding to the elementary Se and ZnSe dissolution are absent as well.

3.3. Voltammetry of CdSe formation process

Solutions based on $CdSO_4$ offer high intrinsic conductivity. So, in this case the electrolytes with the component concentration one order of magnitude less than in the above discussed case were used. For the same reason the stock electrolyte was not used.

Fig. 5 shows cyclic voltammograms of the Ni electrode in the aqueous electrolytes containing Cd^{2+} and SeO_3^{2-} ions. The voltammogram of this electrode in the 0.01 M $CdSO_4$ solution allowed us to determine that the reduction of Cd^{2+} ions by the reaction (e) takes place at the potentials below −0.8 V. The Cd dissolution at the anode polarization occurs at the potentials about −0.3 V. The current peaks associated with the reduction and dissolution of Se (−0.2 B and >0.2 B, correspondingly), CdSe (from −0.5 to −0.6 B and −0.1 B, correspondingly), and Cd (−0.8 B and −0.4 B, correspondingly) are well observed in the voltammograms of the Ni electrode in the 0.01 M $CdSO_4$ + 10^{-5} M SeO_2 electrolyte (pH = 2, and t = 25 °C and 65 °C). When the electrolyte temperature is increased, the potential of the CdSe reduction reaction (d) is shifted into the range of more positive magnitudes. The current maximum associated with the Cd dissolution is absent in the curve related to the lower electrolyte temperature since the potential was scanned only to the range of the metal deposition starting (−0.9 V).

Fig. 6 demonstrates cyclic voltammograms of the bulk n^+ Si electrode in the 0.01 M $CdSO_4$ solution at 25 °C and in the 0.01 M $CdSO_4$ + 10^{-5} M SeO_2 solution (pH = 2, t = 65 °C). We failed to fix in the voltammogram any peak related to the binary compound deposition in the later solution at 25 °C. Referring to Fig. 6, the current maximum associated with the Cd deposition is shifted to the range of more negative potentials as compared with the nickel electrode, and it is located about −0.95 V. The Cd dissolution peak in the reverse cathode branch is shifted as well and it is located about −0.5 V. The plateau in the range of −0.6 V can be associated with the CdSe deposition analogous to the nickel electrode. The low rate of the compound reduction process is explained by the restrictions for the carrier transfer through the silicon/electrolyte interface.

Cyclic voltammograms of the PS electrode in the same solutions are shown in Fig. 7. The voltammogram of the PS electrode in the

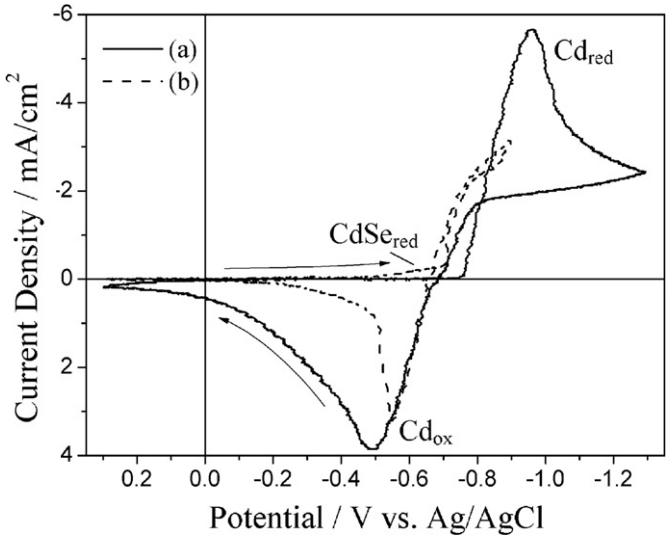

Fig. 6. Cyclic voltammograms of the bulk n^+ Si electrode in following aqueous solutions: (a) 0.01 M $CdSO_4$ at 25 °C, and (b) 0.01 M $CdSO_4$ + 10^{-5} M SeO_2 at 65 °C. The scan rate is 1 V/s.

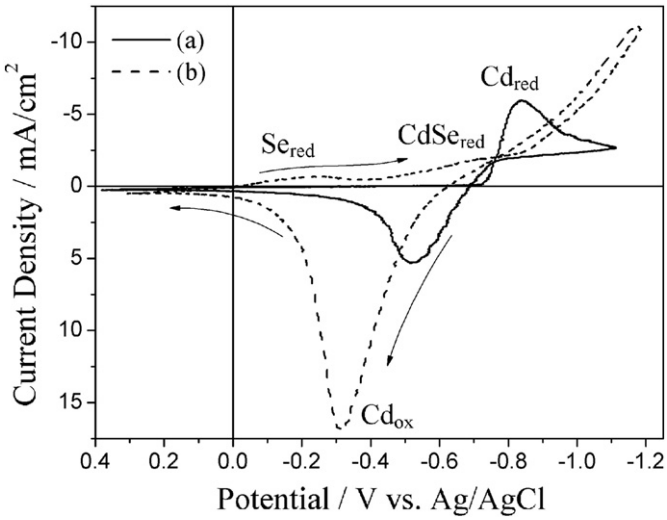

Fig. 7. Cyclic voltammograms of the PS electrode in following aqueous solutions: (a) 0.01 M $CdSO_4$ at 25 °C, and (b) 0.01 M $CdSO_4 + 10^{-5}$ M SeO_2 at 65 °C. The scan rate is 1 V/s.

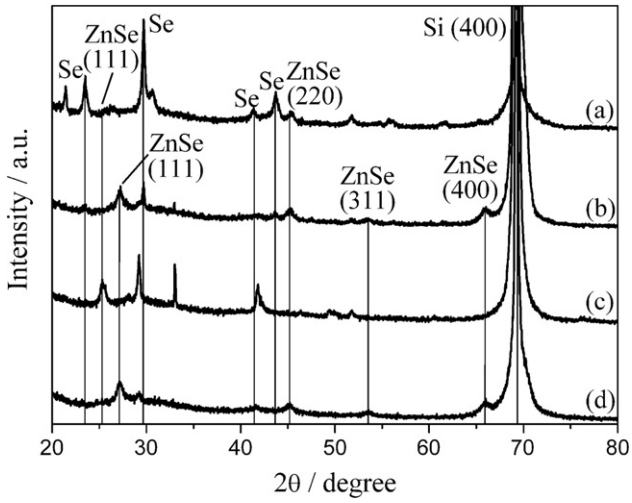

Fig. 8. XRD patterns (CuKα source) of as-deposited and annealed (200 °C in air, 15 min) ZnSe films prepared on PS from the solutions containing 0.2 M $ZnSO_4$ and $5 \cdot 10^{-4}$ M or $5 \cdot 10^{-5}$ M SeO_2 at 85 °C: (a) as-deposited, $5 \cdot 10^{-4}$ M SeO_2, (b) as-deposited, $5 \cdot 10^{-5}$ M SeO_2, (c) annealed, $5 \cdot 10^{-4}$ M SeO_2, and (d) annealed, $5 \cdot 10^{-5}$ M SeO_2.

0.01 M $CdSO_4$ solution at 25 °C is similar to this of the silicon electrode. The Cd reduction and dissolution peaks are located at the potentials of −0.85 and −0.5 V correspondingly. As in the case of the silicon electrode, neither a pronounced peak nor plateau associated with the CdSe reduction are observed in the voltammograms after the addition of 10^{-5} M SeO_2 into the solution at 25 °C. At the temperature of 65 °C, the plateau related to the binary compound deposition appears in the potential range from −0.5 to −0.8 V. The feebly marked peak at −0.25 V corresponding to the Cd deposition onto CdSe is observed.

3.4. Structure and composition of ZnSe and CdSe films on PS

Research by the cyclic voltammetry allowed a potential range of the electrochemical synthesis of ZnSe and CdSe on nickel and silicon substrates to be determined. It is of importance to determine a dependence of the structure and composition of the films formed on the technological parameters (component concentration in the electrolyte, temperature, deposition potential). The variation of these parameters exerts dramatic effect on the deposit quality [9].

X-ray microanalysis of ZnSe films allowed us to determine that the film composition is nearly stoichiometric when the electrolyte temperature is increased to 80–85 °C during the deposition. The ratio of component concentrations in the electrolyte plays a large role for the nickel electrodes while this factor is of little importance for PS electrodes. The deposition potential variation within the range determined by the cyclic voltammetry (from −0.8 to −1.0 V) showed that the most compact deposit of the stoichiometric composition is formed at the potential about −0.85 V. At higher (−0.9 V) potentials, the hydrogen formation is observed resulting in the deposition of films with the rough surface. At lower (−0.8 V) potentials, the deposition takes place non-uniformly all over the surface of the nickel electrode. The deposit formed was amorphous and peeled off mechanically with ease.

When the ZnSe film was deposited on the n^+-type antimony-doped Si (100) substrate of 0.01 Ω·cm resistivity with the mesoporous silicon layer of 65% porosity at the surface from the 0.2 M $ZnSO_4 + 5 \cdot 10^{-4}$ M SeO_2 solution (pH = 2, t = 85 °C) at the potential −0.85 V, the Zn and Se percentage in the ZnSe film was 40% and 60% respectively. For the film deposited on the same substrate from the 0.2 M $ZnSO_4 + 5 \cdot 10^{-5}$ M SeO_2 solution (pH = 2, t = 85 °C), the Zn and Se percentage in the ZnSe film was 46.3% and 53.7% correspondingly. The annealing of ZnSe films on the nickel substrates at 200 °C for 15 min resulted in the 3–10% decrease of the Se share in the deposit. This can be explained by a partial recrystallization of the amorphous compound film and a removal of selenium compounds, specifically, hydrogen selenide H_2Se.

Research by the XRD method showed a dependence of a phase composition of the ZnSe films on the PS substrates on the component concentration in the electrolyte. Curves (a) and (b) on Fig. 8 correspond to the XRD patterns of the ZnSe films deposited on PS at 85 °C

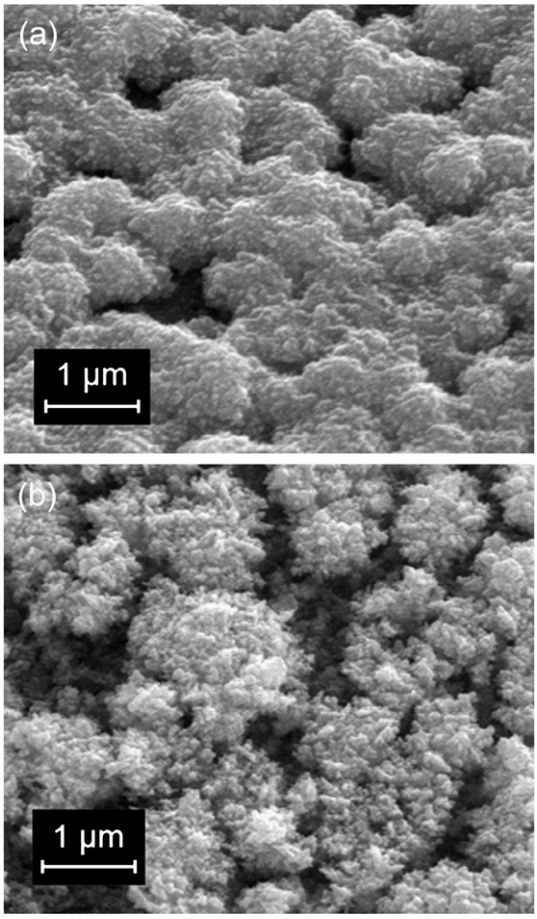

Fig. 9. SEM micrographs of the ZnSe films formed on PS from the aqueous solutions: (a) 0.2 M $ZnSO_4 + 5 \cdot 10^{-4}$ M SeO_2 at 85 °C and (b) 0.2 M $ZnSO_4 + 5 \cdot 10^{-5}$ M SeO_2 at 85 °C.

from the solutions with various concentrations of SeO_3^{2-} ions. The ZnSe films in both cases had mat surfaces and differed in color.

Referring to Fig. 8, curve (a), a high concentration of elementary Se is observed in the ZnSe film deposited on PS from the 0.2 M $ZnSO_4$ + $5\cdot10^{-4}$ M SeO_2 solution at 85 °C. ZnSe crystals are present in small proportion in this film. The decrease of the concentration of selenium-containing ions in the solution resulted in the significant increase of the share of the crystal phase of the binary compound. A presence of several peaks associated with ZnSe crystals of various orientations is indicative of a polycrystalline structure of the film.

Curves (c) and (d) on Fig. 8 correspond to the XRD patterns of the above discussed ZnSe films deposited on PS after the heat treatment at 200 °C in air for 15 min. As may be seen, the intensity of peaks associated with the selenium phases decreased. In the former case, the increase of the ZnSe share in the film took place, probably due to the crystallization of amorphous elementary selenium and zinc with the formation of the binary compound. In the later case, the intensity of peaks related to ZnSe of various crystallographic orientations practically did not change after the heat treatment.

Fig. 9 demonstrates plan view SEM micrographs of the above ZnSe films formed on PS. In both cases the deposition time was 1 h and the thickness of the binary compound layer was approximately 1 μm. As Fig. 9 suggests, ZnSe films formed on PS have the grained porous structure with the grain size about 1 μm. Poor quality of the ZnSe films is dictated by the adsorption rate of the Zn^{2+} ions at the electrode surface [15]. As also evident from the micrographs, the films include clusters of elementary selenium unreacted with zinc during the deposition. At the heat treatment, the number of these clusters decreases.

The CdSe film formed on the PS substrate in the 0.2 M $CdSO_4$ + $5\cdot10^{-5}$ M SeO_2 electrolyte at 80 °C consisted of 48% of Se and 52% of Cd. Fig. 10 shows a XRD pattern of such CdSe film. Referring to Fig. 10, the CdSe film demonstrates a presence of CdSe semiconductor crystals of various crystallographic orientations. So, as in the case of the ZnSe film, the CdSe film deposited on the PS substrate has the polycrystalline structure. However, the peaks associated with elementary selenium are absent in the XRD pattern. Moreover, the CdSe film showed a smooth mirror surface.

In accordance with the results of X-ray microanalysis, the element composition of CdSe films formed on the mesoporous silicon layers of 65% porosity weakly depends on the deposition potential from the range determined by the cyclic voltammetry. However, the composition of the deposits is nearest to stoichiometric at the deposition potential of −0.6 V. At the same time, the concentration of the selenium-containing ions in the electrolyte plays a large role. Se excess

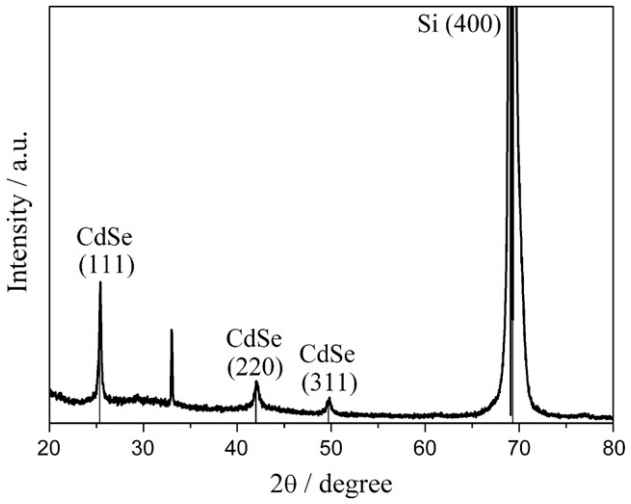

Fig. 10. XRD pattern (CuKα source) of the CdSe film deposited on PS from the 0.2 M $CdSO_4$ + $5\cdot10^{-5}$ M SeO_2 aqueous solution at 80 °C.

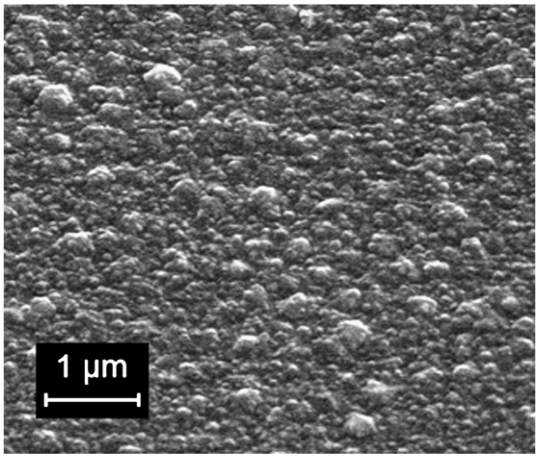

Fig. 11. SEM micrograph of the CdSe film formed on PS from the 0.2 M $CdSO_4$ + $5\cdot10^{-5}$ M SeO_2 aqueous solution at 80 °C.

can be avoided only with low enough ($\leq 5\cdot10^{-5}$ M) SeO_2 concentrations. The increase of the electrolyte temperature to 80–85 °C also allows the metal concentration in the deposit to be increased.

Fig. 11 demonstrates the SEM micrograph of the CdSe film. The thickness of the formed film was approximately 1 μm and the deposition time was 1 h. As seen in Fig. 11, the CdSe film is more compact, and its surface is considerably smoother than in the case of the ZnSe films. This feature is dictated by better adhesion of Cd^{2+} ions to the electrode surface during the deposition.

4. Conclusions

Research into the electrochemical deposition process of ZnSe and CdSe compound semiconductors from aqueous acid solutions showed that synthesis of these selenides takes place practically equally on metal, silicon, and PS substrates in accordance with theory. There are no difficulties concerned with either the surface condition of silicon or the potential barrier at the semiconductor/electrolyte interface for the ZnSe deposition. But CdSe can be formed on the bulk silicon and PS only at the elevated temperature.

For the ZnSe film deposition onto the PS substrates, the ratio of metal and chalcogen ions in the electrolyte may be the same as for the deposition on the metal substrates. When the CdSe films are deposited onto PS, the concentration of selenium-containing ions in the electrolyte should be one order of magnitude less to avoid a significant excess of chalcogen in the deposit. The electrolyte temperature is also of critical importance. The temperature should be no less than 80 °C to provide optimal conditions for the binary compound formation.

The potentials range of the electrochemical deposition of the ZnSe films onto PS is quite narrow. Polycrystalline ZnSe films may be formed at the potential of 0.85 ± 0.025 V relative to the reference AgCl electrode. For the CdSe deposition, this range is wider. In the potential range from 0.5 to 0.6 V, binary compound films of the same quality with the composition close to stoichiometric are formed.

The surface morphology and the phase composition of the chalcogenide films strongly depend on the adhesion of metal involved. In the case of the CdSe deposition, compact films with the smooth surface are formed. The ZnSe films deposited onto PS have the rough grained surface and contain a great number of elementary Se. the heat treatment at 200 °C in air allows the Se content in the ZnSe films to be reduced.

Acknowledgments

The work has been supported by the Belarus Government Research Program “Nanomaterials and nanotechnologies,” grant 6.12.03.

The authors would like to thank V. Tzibulsky for his help in obtaining SEM images and V. Yakovtseva for the helpful discussions and valuable advises.

References

[1] A.P. Samantilleke, M.H. Boyle, J. Young, I.M. Dharmadasa, J. Mater. Sci. Mater. Electron. 9 (1998) 231.
[2] R. Tena-Zaera, M.A. Ryan, A. Katty, G. Hodes, S. Bastide, C. Lévy-Clément, C.R. Chimie 9 (2006) 717.
[3] S. Hasegawa, K. Maehashi, H. Nakashima, T. Ito, A. Hiraki, J. Cryst. Growth 95 (1989) 113.
[4] V. Levchenko, L. Postnova, V. Bondarenko, N. Vorozov, V. Yakovtseva, L. Dolgyi, Thin Solid Films 348 (1999) 141.
[5] V. Yakovtseva, N. Vorozov, L. Dolgyi, V. Levchenko, L. Postnova, M. Balucani, V. Bondarenko, G. Lamedica, E. Ferrara, A. Ferrari, Phys. Status Solidi, A 182 (2000) 195.
[6] V. Raiko, R. Spitzl, J. Engermann, V. Borisenko, V. Bondarenko, Diamond Relat. Mater. 5 (1996) 1063.
[7] D. Lincot, Thin Solid Films 487 (2005) 40.
[8] M. Bouroushian, T. Kosanovic, Z. Loizos, N. Spyrellis, J. Solid State Electrochem. 6 (2002) 272.
[9] L. Beaunier, H. Cachet, M. Froment, G. Maurin, J. Electrochem. Soc. 147 (2000) 1835.
[10] S. Süzer, S. Kutun, F. Kadirgan, Fresenius' J. Anal. Chem. 355 (1996) 384.
[11] M. Neumann-Spallart, C. Königstein, Thin Solid Films 265 (1995) 33.
[12] S. Nakamura, Jpn. J. Appl. Phys. 44 (2005) 1939.
[13] M. Bouroushian, J. Charoud-Got, Z. Loizos, N. Spyrellis, G. Mourin, Thin Solid Films 381 (2001) 39.
[14] F. Jackson, L.E.A. Berlouis, P. Rocabois, J. Cryst. Growth 159 (1996) 200.
[15] C. Natarajan, M. Sharon, C. Lévy-Clément, M. Neumann-Spallart, Thin Solid Films 237 (1994) 118.
[16] M. Bouroushian, J. Charoud-Got, Z. Loizos, N. Spyrellis, J. Mater. Sci. Lett. 19 (2000) 2201.